RESEARCH ARTICLE

The performance of chitosan/montmorillonite nanocomposite during the flocculation and floc storage processes of *Microcystis aeruginosa* cells

Zhiyuan Wang[1] · Chao Wang[1] · Peifang Wang[1] · Jin Qian[1] · Jun Hou[1] · Yanhui Ao[1] · Baohai Wu[1]

Abstract This study aimed to investigate the performance of chitosan-modified nano-sized montmorillonite (CTS/NMMT) during the flocculation of *Microcystis aeruginosa* (MA). The release of intracellular microcystins (MCs) caused by the damage of intact MA cells during the flocculation and floc storage processes was also comprehensively evaluated through scanning electron microscopy (SEM) and measurement of K^+ and Mg^{2+} release. With the application of the Box–Behnken experimental design combined with response surface methodology, the quadratic statistical model was established to predict and optimize the interactive effects of content of CTS/NMMT, weight ratio of NMMT to CTS, and agitation time on the removal efficiency of MA cells. A maximum removal of 94.7 % MA cells was observed with content of CTS/NMMT 300–320 mg L^{-1}, weight ratio of NMMT to CTS 14–16, and agitation time 16–50 min. During the flocculation process, CTS/NMMT aggregated MA cells as flocs and served as a protection shield for cells. The extracellular and intracellular microcystin–leucine–arginine (MC-LR) decreased remarkably and the yield of intracellular MC-LR showed a decreasing trend during the flocculation. The cell integrity was slightly damaged by the mechanical actions rather than by the flocculant. During the floc storage process, cell lysis and membrane damage were remarkably aggravated. The noticeable increase of K^+ and Mg^{2+} release indicated that CTS/NMMT damaged the integrity of most MA cells in the flocs and liberated the intracellular MC-LR. Meanwhile, NMMT and CTS polymers assisted the adsorptive removal of extracellular MC-LR released to water. The flocs should be timely treated within 12 h to prevent the leakage of MCs.

Keywords Chitosan/montmorillonite nanocomposite · *Microcystis aeruginosa* · Flocculation · Floc storage · Microcystin-LR release · Cell lysis

✉ Peifang Wang
pfwang2005@hhu.edu.cn

Zhiyuan Wang
zhiyuan.wang1988@hotmail.com

Chao Wang
cwang@hhu.edu.cn

Jin Qian
hhuqj@hhu.edu.cn

Jun Hou
hhuhjyhj@126.com

Yanhui Ao
andyao@hhu.edu.cn

Baohai Wu
hjywbh@hhu.edu.cn

[1] Key Laboratory of Integrated Regulation and Resource Development on Shallow Lakes, Ministry of Education, College of Environment, Hohai University, No. 1 Xikang Road, Nanjing 210098, China

Introduction

Harmful cyanobacterial blooms have increasingly occurred worldwide, and the effective removal or inhibition of the algal blooms becomes critically important. *Microcystis aeruginosa* (MA), as one of the most dominant cyanobacterial species in the algal blooming, can produce intracellular metabolites, such as microcystins (MCs), taste- and odor-causing substances, and other organic matters into water (Zhou et al. 2013). Under the effect of anthropogenic pollution, the production of highly hepatotoxic MCs is enhanced with the stimulated growth of MA and can cause serious liver disease (Carmichael 2001; Polyak et al. 2013). Microcystin–leucine–arginine (MC-LR) has been identified as the most fatal

and commonly occurring toxin among the molecular variants of MCs isolated so far (Campos and Vasconcelos 2010; Thirumavalavan et al. 2012). A provisional safety guideline of 1.0 μg L^{-1} MC-LR in drinking water has been recommended by the World Health Organization (Yan et al. 2006).

Flocculation has been intensively studied on the removal of HABs for its extremely low cost and high efficiency (Hua et al. 2006). Traditional flocculants such as ferric chloride (FeCl$_3$), aluminum chloride (AlCl$_3$), and polyacrylamide (PAM) may lead to the increase in metal concentration in water, which may cause human health implications or the dispersion of acrylamide oligomers which may also be health hazards (Dong et al. 2014). Modified clays display higher adsorption capacity than original clays and frequently exhibit remarkably improved mechanical and material properties (Wang and Wang 2007).

Chitosan (CTS) is known to be a non-toxic, easily acquirable and biodegradable flocculant (Renault et al. 2009; Zeng et al. 2008). Its application for the adsorption of mineral colloids, heavy metal ions, and organic matters from aqueous solution in an industrial scale has been investigated (Chen and Chung 2011; Wan Ngah et al. 2011). The presence of amino and hydroxyl groups of CTS shows powerful adsorptive capacity as a flocculating agent to harvest cyanobacterial cells from cultures (Farid et al. 2013). Nano-sized montmorillonite (NMMT) K10, as a type of synthetic bentonite clay activated with mineral acid, has been proved cost-effective for the adsorption of MC-LR (Wang et al. 2014). However, its low flocculation rate and requirement of high loadings are unacceptable for industrial use (Pan et al. 2006a). The NMMT modified with polysaccharides is more uniformly dispersed and has higher specific surface area and weaker bonds between layers, which provide outstanding flocculation and adsorption ability (Wan Ngah et al. 2011).

Modification on netting and bridging properties of clays by CTS can dramatically promote the flocculation of MA cells in freshwater (Hua et al. 2006; Shao et al. 2012). CTS-modified clays were certified as non-harmful to human and animals (Pan et al. 2006a). CTS-clay composites can be regenerated and reused in many cycles of adsorption with resilience and lowest loading (Auta and Hameed 2014). The CTS/NMMT biopolymer nanocomposites frequently display remarkable improved mechanical and material properties and attract considerable interest in the field of polymer science (Wang and Wang 2007). To date, the performance of the CTS/NMMT nanocomposite on the removal of MA cells during the flocculation and the floc storage has not been systematically assessed.

A statistically based Box–Behnken experimental design and response surface methodology (RSM) has proved to be an effective approach, which is frequently used to identify synergic effects and predict values of significant process variables from a large number of potential variables with a minimum of optimized combination experiments (Kumar and Phanikumar 2013; Zhang et al. 2015). The effect of dosage, fraction of organic matter, and reaction time of modified clays on the flocculation has been individually studied by employing the conventional one-factor-at-a-time method (Li et al. 2014; Pan et al. 2006b; Shao et al. 2012). However, previous studies ignored the determination of the simultaneous effects on the flocculation capacity of specific flocculants and the optimization of experimental factors in MA removal by adopting a full range of response surface methodology.

The chemical stress to the cell membrane and the cell damage caused by the mechanical action in the chemical treatment progress have been discussed before (Jančula and Maršálek 2011). Differently, the application of some traditional chemical agents at appropriate contents did not cause toxin release (Ho et al. 2012). The mechanisms underlying cell viability and toxin release involved in the floc storage process of MA have drawn little attention until recently (Li et al. 2014). Extracellular MC-LR has been found difficult to be removed by traditional water treatments (Zhou et al. 2013). Since the clarification/filtration treatments are inefficient for the removal of MCs, the sludge supernatant containing MCs recycled to the former water treatment progress would be problematic (Pei et al. 2014). Thus, experimental strategies should focus on evaluating the leakage of intracellular MCs and seeking an effective method of avoiding the side effects of special flocculants on the integrity of MA cells and the secondary pollutions during the flocculation and floc storage process.

In this research, the removal responses of MA cells during the CTS/NMMT flocculation process were investigated through the RSM with the aim of optimizing the controlling parameters to achieve the maximum flocculation efficiency. By performing a batch of Box–Behnken-designed experiments, we established the statistical response surface model to predict the interactive effects of content of CTS/NMMT, weight ratio of NMMT to CTS, and agitation time on the flocculation efficiency of MA cells by the CTS/NMMT nanocomposite. The MA growth and the intracellular and extracellular MC-LR concentrations in different growth stages were also assessed. The relation between cell integrity and intracellular toxin release was further evaluated by scanning electron microscopy (SEM) analysis and measurements of K$^+$ and Mg^{2+} release. The impacts of CTS/NMMT on the control of MC-LR release related to the cell damage during the flocculation and the floc storage were studied.

Materials and methods

Algal culturing

The axenic strain of *M. aeruginosa* (FACHB-905) was kindly supplied from the Institute of Hydrobiology, Chinese Academy of Sciences (Wuhan, China), and used as model algae in this study. This toxic cyanobacterial strain was isolated from Dianchi Lake, China, in 1998. The algal cultures were incubated in BG11 medium under 25 °C with 2500 lx illumination under a light/dark photoperiod of 12/12 h. The autoclaves (MLS-3750, Sanyo™, Japan) were used at 120 °C (1.2 atm) for 2 h as aseptic techniques to minimize additional bacterial contamination of containers. The algal cultures were harvested at different growth phases to obtain the desirable initial densities and centrifuged at 8000 rpm for 10 min.

The natural water was sampled from Taihu Lake (Jiangsu Province, China), where large-scale harmful algal blooms characterized by the dramatically increasing abundance of MA cells could be constantly observed in summer. The TN, TP, and pH were respectively 2.20 mg L^{-1}, 0.12 mg L^{-1}, and 7.15. The water samples were filtered through 500-mesh (25 μm) sieves and 0.45-μm glass fiber membranes to decrease the grazing effect of zooplanktons, aquatic plants, and other suspended matters. These samples were used for batch experimental treatments within 6 h.

Preparation of CTS-modified NMMT

Nano-sized MMT K10 with 95 % purity and CTS was purchased from Liaoyuan 4S-tech Co., Ltd., Nanjing, China. The modification of NMMT with CTS was conducted according to the method described by Hua et al. (2006). Milli-Q deionized water was supplied by Millipore™ water purification system (Bedford, MA, USA). One hundred milliliters of NMMT suspension (10 mg mL^{-1}) was prepared with deionized water in a thermostated magnetic stirrer (Guohua® 85-2, Changzhou, China) for 2 h at room temperature. One hundred milligrams of CTS was dissolved with 10 mL of 1 % HCl as the soluble hydrochloride salt (CTS-HCl) and diluted with deionized water to obtain the stock solution with a fixed concentration of 1 mg mL^{-1}. To modify the clays, a certain volume of CTS stock solution was slowly added into the NMMT suspension to obtain nanocomposites with different feed compositions of NMMT to CTS according to the Box–Behnken experimental matrix. The mixture was agitated vigorously for 2 h at 70 °C, dried in an oven at 70 °C to a constant weight, milled, and sieved through a 300-mesh screen. All CTS/NMMT nanocomposite samples ready for use in the flocculation experiments had a particle size of <0.2 mm.

Measurement of extracellular and intracellular MC-LR concentrations

The extraction of extracellular and intracellular MC-LR referred to the method of Hu et al. (2014). Twenty milliliters of MA solution was separated in a centrifuge (H2050R-1, Xiangyi™, Hunan, China) at 10,000 rpm at 4 °C for 10 min. The supernatant was filtrated through a 0.22-μm Whatman GF/C glass fiber membrane. The MC-LR concentration in the filtrate represented the concentration of extracellular MC-LR. The MA cells harvested by the membrane were rinsed in deionized water, dissolved in 5 % acetic acid solution, and ultrasound-treated for 30 min with an ultrasonic disruptor (KQ3200DE, Shumei®, China). The completely lyophilized cells were dispersed in deionized water and subjected to three freeze/thawing cycles at −70 °C in liquid nitrogen prior to centrifuge separation and filtration through methanol-activated solid-phase extraction (SPE) cartridges (500 mg/6 mL, CNWBOND® LC-C18, ANPEL™, Shanghai, China) at a minimum speed of 1 mL min^{-1}. The eluent was collected, dried under nitrogen at 40 °C, and adjusted to a constant volume of 0.5 mL using HPLC-grade methanol. The MC-LR concentration in the extract represented the concentration of intracellular MC-LR.

Both extracellular and intracellular MC-LR concentrations were measured by the HPLC system as reported in our previous study (Wang et al. 2014). The HPLC system comprised a Waters Alliance e2695 separations module (Waters® Corporation, Milford, MA, USA) with a Waters 2489 UV/Visible detector, a Waters 2998 photodiode array detector, an inline vacuum degasser, a quaternary mixing pump, a thermostated autosampler, and a heated column compartment. The wavelength was set to 238 nm. The separation was achieved on an XBridge LC C18 5 μm, 4.6 mm×150 mm HPLC column (XBridge Systems, Inc., Mountain View, CA, USA). The detection limit of MC-LR concentration is 0.1 ng mL^{-1} with the S/N ratio of 3. The injection volume was 10 μg L^{-1} with a flow rate of 0.6 mL min^{-1}. The mobile phase consisted of 0.1 % formic acid in water (solvent A, 40 %) and 0.1 % formic acid in HPLC-grade methanol (solvent B, 60 %). HPLC-grade methanol and formic acid were obtained from Tedia (OH, USA) and Merck (Germany), respectively. MC-LR standard was purchased from Agent Technology (Switzerland) and stored below −25 °C. The standard curve (R-squared> 99.9 %) was obtained for MC-LR concentrations ranging from 1 to 1000 μg L^{-1} to ensure minimal system error.

Measurement of K$^+$ and Mg^{2+} release

To measure the K$^+$ and Mg^{2+} leaking from MA cells as described before (Zhang et al. 2011; Zhou et al. 2013), 10 mL supernatant sample was filtrated through a 0.22-μm Whatman GF/C glass fiber membrane and acidified to pH<2 with HNO$_3$

(analytical grade, Liaoyuan 4S-tech Co., Ltd., Nanjing, China). The K^+ and Mg^{2+} concentrations were measured by inductively coupled plasma mass spectrometry (ICP/MS) using an Agilent 7500a system (Agilent® Technologies Inc., CA, USA). The fraction of K^+ and Mg^{2+} release was calculated as

$$\text{Release} = \frac{C_t - C_{ct}}{C_{ct} - C_0} \times 100\% \qquad (1)$$

where C_t is the K^+ and Mg^{2+} concentration in the flocculation system at time t, C_{ct} is the maximum K^+ and Mg^{2+} concentration in the control sample at time t, and C_0 is the K^+ and Mg^{2+} concentration in BG11 culture without MA cells.

Box–Behnken experimental design for the optimization of flocculation

The Box–Behnken response surface model was used for the experimental design to evaluate the interactive effects of the significant operating parameters and to optimize the MA flocculation on the CTS/NMMT nanocomposite. The three main controlling parameters, content of CTS-modified NMMT (100–500 mg L^{-1}), weight ratio (wr) of NMMT to CTS (1–20), and agitation time (10–120 min), were chosen as model variables to study their interactive effects on the flocculation process. The ranges of parameters were selected based on preliminary experiments. Each independent actual parameter was varied over three coded levels (−1, 0, +1), which composed the batch experimental design matrix derived from the Box–Behnken design summarized in Table 1. The removal efficiency (%) of MA cells by CTS/NMMT under different

experimental combinations based on this matrix was estimated as the model responses.

The true value of each selected variable i was coded as follows:

$$x_i = \frac{X_i - X_{ci}}{\Delta X_i}, i = 1, 2, 3, \ldots, k \qquad (2)$$

where x_i is the coded level, X_i is the real value of an independent variable, X_{ci} is the real value of an independent variable at the central point, and ΔX_i is the step change of variable i.

These independent factors were represented as process variables in a quantitative form:

$$Y = f(A, B, C) \qquad (3)$$

where Y is the predicted response of cell removal efficiency (%) and A (CTS/NMMT content), B (wr of NMMT to CTS), and C (agitation time) are the coded levels of the actual variables.

The response values were firstly approximated by a suitable linear polynomial, and then the quadratic, cubic, and higher order polynomial. In the system with curvature, the second-order polynomial in the form of a quadratic model showed the best fit with our experimental data:

$$Y = k_0 + k_1 A + k_2 B + k_3 C + k_{12} AB + k_{13} AC + k_{23} BC$$
$$+ k_{11} A^2 + k_{22} B^2 + k_{33} C^2 \qquad (4)$$

where k_{ij} are the estimated coefficients of the equation.

A total of 16 different experimental combinations (including 4 replicates of the center point for error estimation) was

Table 1 Box–Behnken experimental design matrix of three variables (content of CTS-modified NMMT, weight ratio of NMMT to CTS, and agitation time) and the experimental responses

Run	Variables			Removal efficiency (%)
	Content (mg L^{-1})	Weight ratio of NMMT to CTS	Time (min)	
1	100	1	65	65.3
2	100	10.5	10	77.3
3	100	10.5	120	66.1
4	100	20	65	74.9
5	300	1	10	80.0
6	300	1	120	78.5
7	300	10.5	65	93.2
8	300	10.5	65	92.7
9	300	10.5	65	94.1
10	300	10.5	65	93.6
11	300	20	10	92.3
12	300	20	120	88.1
13	500	1	65	69.9
14	500	10.5	10	79.2
15	500	10.5	120	75.6
16	500	20	65	78.4

designed for calculation of the 10 coefficients of the second-order polynomial equation to approximate the experimental values, which were derived from the standard Box–Behnken model established by Design Expert® (DX) 8.0.6 (Stat-Ease Inc., Minneapolis, MN, USA). The determination of the complex response surface provided by relatively few combinations of variables was obtained by plotting the expected response values.

Flocculation experiments were conducted according to the experimental design matrix in 1-L glass beakers using a rate-controlled jar test apparatus (JJ-4A, Jiapeng®, Shanghai, China) rated at 25 rpm. The MA culture was harvested with an initial density of 1.2×10^5 cells mL^{-1} at day 2 of the logarithmic growth phase and resuspended in natural water samples collected from Taihu Lake. Up to six flocculation samples were placed simultaneously on the gang stirrer and the flocculant was slowly added. After the flocculation process, each sample was settled for 60 min.

The supernatant sample was collected at 1 cm below the surface for the microscopic analysis of cell density. The sample was fixed with 1 % Lugol's solution for 24 h and adjusted to a constant volume with deionized water. Cell numbers were enumerated at the species level by observing the hemocytometer slide under a standard compound (upright) microscope (Axioskop 40 Pol, Carl Zeiss™ Light Microscopy, Germany) at ×400–×1000 magnification. The cell numbers that were counted from colonies and single cells were then converted to density with the aliquot size, and the density was expressed as cell number per milliliter. The count precision was ±10 %, assuming that the cells were randomly distributed (Venrick 1978).

Flocculation experiments for different growth phases

MA cells were harvested at three initial algal densities: $1.28 \pm 0.13 \times 10^5$, $2.64 \pm 0.12 \times 10^6$, and $5.11 \pm 0.12 \times 10^7$

cells mL^{-1}. The low initial density of $1.28 \pm 0.13 \times 10^5$ cells mL^{-1} and the medium initial density of $2.64 \pm 0.12 \times 10^6$ cells mL^{-1} represent the logarithmic growth phase at day 2 and day 6, and the high initial density of $5.11 \pm 0.12 \times 10^7$ cells mL^{-1} represents the earlier stationary phase at day 10. The selected initial algal densities used in this study were comparable to those usually observed in a natural algal bloom. Appropriate amounts of CTS-modified NMMT were added to MA samples incubated with the culture medium in 1-L glass beakers to perform flocculation experiments under the optimum flocculation conditions assessed by the response surface methodology. The MA samples without flocculants served as the controls to prevent false positives.

The CTS/NMMT samples before and after flocculation were dehydrated through a series of ethanol solutions and dried with a vacuum drier. The completely dried samples were mounted on the copper stub, coated with gold powders, and drawn for scanning electron microscope (SEM) analysis (Hitachi® S-4800, Japan). The SEM images were captured at various magnifications with an electron beam (high accelerating voltage of 18 kV) at a 45° tilt on the left side.

Statistical analysis

The statistical significances of Box–Behnken response surface modeling parameters and their interactions (combinations of two codes) at various levels of probability values were checked by Student's t test and p-values. The t value represents the ratio of the estimated parameter effect to the estimated parameter standard error. A large magnitude of t value represents the statistical significance of the corresponding variable in the regression model (Yetilmezsoy and Saral 2007). The

Table 2 Estimated coded parameters of the response surface model and their statistical significance

| Variables	Parameter coefficient	Mean square	Standard error	t value	F value	p value > F
Intercept	93.20					
A	2.44	47.53	0.49	4.98	24.61	<0.01
B	5.00	200.00	0.49	10.20	103.57	<0.01
C	−2.56	52.53	0.49	−5.22	27.20	<0.01
AB	−0.28	0.30	0.69	−0.41	0.16	0.70*
AC	1.90	14.44	0.69	2.75	7.48	0.03
BC	−0.67	1.82	0.69	−0.97	0.94	0.36*
A^2	−15.63	1027.96	0.68	−22.99	532.33	<0.01
B^2	−5.45	125.06	0.68	−8.01	64.76	<0.01
C^2	−3.02	38.53	0.68	−4.44	19.95	<0.01

*p>0.05, non-significant parameter
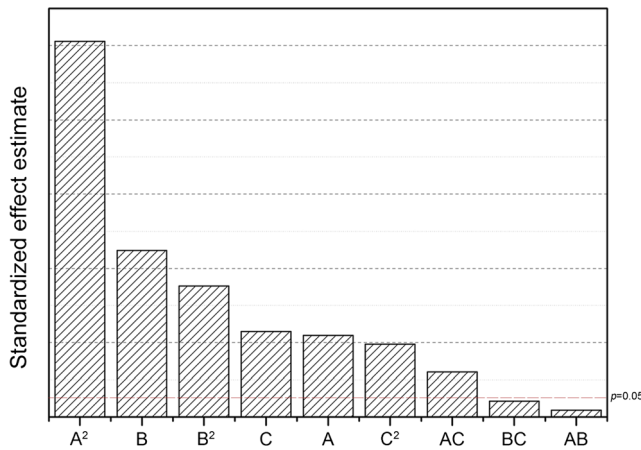
Fig. 1 Pareto chart showing the standardized effects of variables on the MA flocculation efficiency

standardized effects of the variables based on the t values of the independent variables and their interactions are shown as a Pareto chart. The length of each bar in the Pareto chart indicates the standardized effect of that variable on the response, and the alpha level of 0.05 was used to determine the statistical significance (Yetilmezsoy and Saral 2007). A small p value ($p < 0.01$) indicates a statistically significant parameter effect, and a term with $p > 0.05$ was considered non-significant in this study.

The modeling experimental data were subjected to the analysis of variance (ANOVA) to test the accuracy and applicability of the response surface model. The significance of the response surface model was checked by the probability value and Fisher F test. The goodness of the regression model was checked by the coefficient of variation (CV) and coefficient of R-squared. The model precision was elucidated by the signal-to-noise ratio, which compares the range of predicted values at the design points to the average prediction error. All information on the lack of fit contained in the residuals was reflected by the normal probability

plot and parity plot of residuals to check the model adequacy (Liu et al. 2004b).

Results and discussion

Response surface modeling for MA flocculation optimization

The response surface model was established as an effective means of reflecting the MA cell removal efficiency affected by the controlling parameters. The statistical significances of parameters and their interactions at various levels of probability values are shown in Table 2. The standardized effects of the variables on the MA flocculation efficiency based on the t values of the independent variables and their interactions are shown as a Pareto chart in Fig. 1. High values of the parameter estimates for these variables with high levels of significance indicated their importance in the flocculation process.

The selected first-order and second-order parameters were shown to be statistically significant except for the interactive parameters AB and BC, because the Pareto bars for these two parameters remain outside the reference line and their p values are relatively high. The quadratic term for content of CTS-modified NMMT (A^2) was found as the most significant component of the regression model (estimated coefficient$=-15.63$, $t=-22.99$, $F=532.33$, $p < 0.01$) for the present application. Among the controlling parameters, it was clear that the linear term for weight ratio of NMMT to CTS (B) had the most significant effects on removal efficiency (estimated coefficient$=5.00$, $t=10.20$, $F=103.57$, $p < 0.01$). Only variables A, B, and AC showed a significant positive relationship with the removal efficiency, while all other variables had negative effects.

By fitting the parameter coefficients estimated by RSM based on the Box–Behnken design (Table 2) and

Table 3 ANOVA for the Box–Behnken response surface model

Sources of variation	Sum of squares	Degree of freedom	Mean square	F value	p value $> F$
Model	1585.26	9	176.14	91.21	<0.01
Residual	13.52	7	1.93		
- Lack of fit	13.52	3	4.51		
- Pure error	0	4	0		
RMSE	1.39	R-squared		0.9915	
Mean	81.86	Adjusted R-squared		0.9807	
CV* (%)	1.70	Predicted R-squared		0.8647	
		Adequate precision		27.01	

*CV = RMSE/mean

**Fig. 2** Normal probability plot of residuals
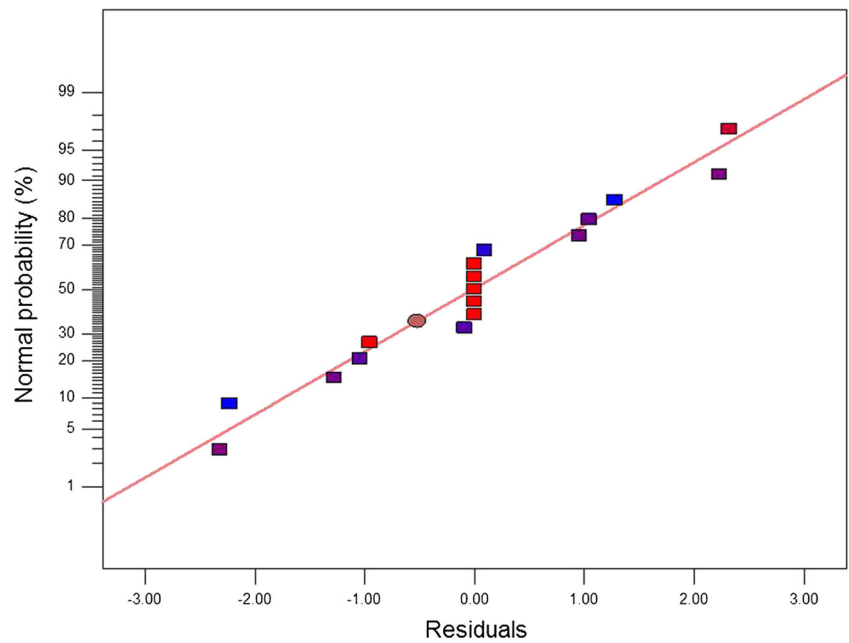
emphasizing the most significant polynomial terms, the final second-order regression equation in terms of coded factors to describe the MA cell removal efficiency during the flocculation process of MA cells by CTS-modified NMMT was

$$Y = 93.20 + 2.44A + 5.00B - 2.56C - 0.28AB + 1.90AC - 0.67BC - 15.63A^2 - 5.45B^2 - 3.02C^2 \tag{5}$$

The coded response values of the independent variables were entered into the established design to fit the suggested numerical model.

The ANOVA results in Table 3 show that the regression model was significant, because of the low probability value ($p < 0.01$) and the high Fisher F test value (91.21), which means that there is only a 0.01 % chance that a model F value this large could occur because of noise. The pure error of zero indicates that the lack of fit was not significant. The goodness of regression was also verified by the low coefficient of variation and the high coefficients of R-squared, which indicates the high dependence between the observed and the simulated response values. The relatively high value of model precision (27.01) indicates a satisfactory model discrimination and an authentic relationship between the model responses and

Fig. 3 Parity plot showing the correlation between the predicted and experimental values
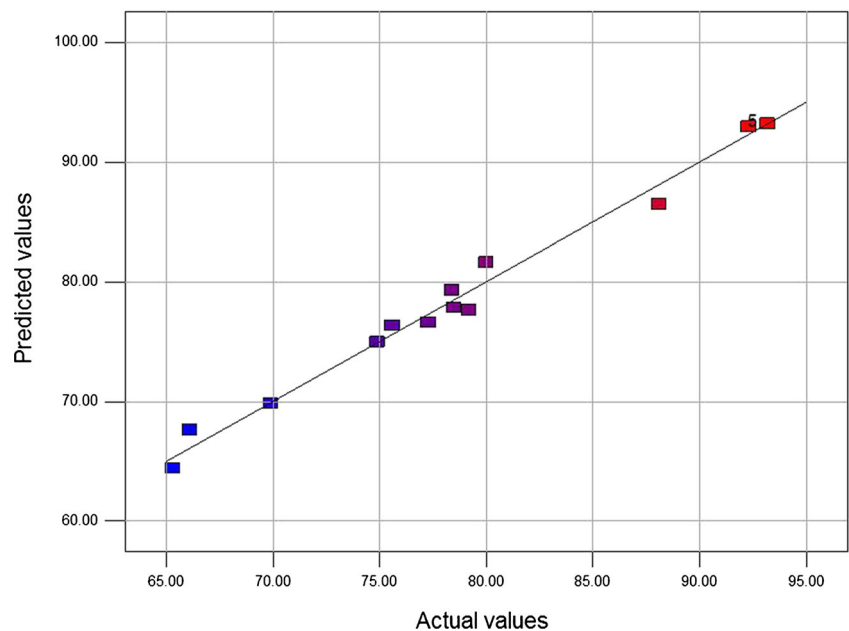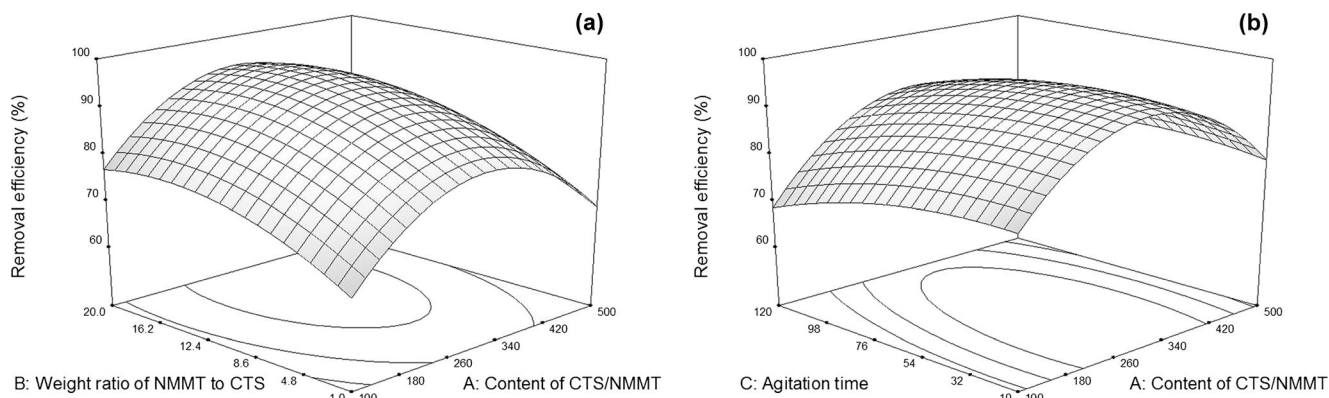
Fig. 4 3D Box–Behnken response surface plots of *Microcystis aeruginosa* flocculation by CTS/NMMT as a function of content of CTS/NMMT–weight ratio of NMMT to CTS (**a**) and content of CTS/NMMT–agitation time (**b**)

significant variables. The normal probability plot of residuals (Fig. 2) is a graphical diagnostic tool, which confirms the assumptions that errors are normally distributed and error variances are homogeneous. The parity plot depicted in Fig. 3 shows the satisfactory correlation between the predicted and observed values of flocculation efficiency. As indicated by the points clustering around the diagonal line, no serious deviation between observed and predicted values is indicated (Imandi et al. 2007). Therefore, this regression model fits to predict the removal efficiency of MA cells and analyze the response patterns for optimization.

Interactive effects of variables on MA flocculation

By changing two variables within their experimental ranges and keeping the other variable at its optimum level, the RSM provided the response surface plots and corresponding contour plots to explain the interactions among the flocculation parameters and the regular pattern of experimental data variances. The predicted responses were plotted according to the final quadratic polynomial equation. Graphical optimization of the response surface plots was conducted with DX analysis to determine the range of the optimal condition that maximizes the removal efficiency of MA cells.

The interactive effect of CTS/NMMT content and wr of NMMT to CTS is shown in Fig. 4a. At fixed agitation time,

the removal efficiency initially increased to as high as 94.9 % and then decreased slightly with increasing content of CTS/NMMT from 100 to 500 mg L^{-1}. Similarly, increasing wr of NMMT to CTS from 1 to 14 facilitated the cell removal, but restrained the flocculation from 16 to 20. The interactive effect of content of CTS/NMMT and agitation time is shown in Fig. 4b. With low and high contents of CTS/NMMT, the removal efficiency increased with agitation time increasing from 10 to 16 min and decreased afterward with the further increment of agitation time from 50 to 120 min. The maximum removal efficiency was observed with content of CTS/NMMT 300–320 mg L^{-1}, wr of NMMT to CTS 14–16, and agitation time 16–50 min.

The modeling results could be interpreted as follows. The quadratic variable of the content of CTS/NMMT (A^2) has the highest coefficient with a negative value. The flocculant at low content removes preferentially the hydrophobic material rather than the hydrophilic MCs (Li et al. 2014). The positively charged CTS acted as an effective participant for the removal of negatively charged MA cells by charge neutralization (Dong et al. 2014). The increasing content of CTS/NMMT, however, could reduce the removal efficiency because of the destabilization caused by the excess cationic charges. As a long-chain polymer, CTS performs a netting and bridging mechanism between algal cells and could thus reshape cell flocs, whereas clays also play important roles in the sedimentation of the flocs (Shao et al. 2012). Clays such as

Table 4 Results of validation experiments under optimum conditions

Test	Variables			Removal efficiency (%)		
	Content (mg L^{-1})	NMMT/CTS	Time (min)	Predicted value	Experimental value	Standard deviation
1	300	15	38	95.3	94.4	±0.7
2	310	15	50	94.9	93.8	±1.3
3	310	16	38	95.2	94.1	±1.2
4	310	14	40	94.8	94.6	±2.1
5	320	15	42	95.2	94.7	±0.5

montmorillonite are usually negatively charged in natural freshwater, and hence, the mechanism of electrostatic neutralization would not contribute significantly to the aggregation between clay particles and MA cells. However, the netting and bridging modification using CTS, which is environmentally benign and biodegradable, could turn NMMT into an effective MA scavenger.

The related field of the response surface revealed that the weight ratio of NMMT to CTS exerted a marked favorable effect in the flocculation. Student's t values and p values suggested by the model pointed out that the weight ratio of NMMT to CTS with the highest coefficient was the most significant actual parameter. The fibrous solids like NMMT could serve as the frames and weights to the network built by CTS between algal cells, which is the effective settling of MA flocs (Pan et al. 2006b). The removal efficiency of MA cells can be considerably reduced with a large fraction of clay in the CTS/NMMT with the charge neutralization playing the dominant role, while the unfolding of the molecular chain would be prevented and the netting and bridging property are thereby weakened. The flocculation capacity would also be restrained while the amount of intercalated CTS is saturated. Accordingly, only an appropriate NMMT dosage brings a better removal efficiency of MA cells, which is the most critically important parameter for the application of the clay/soil technique in freshwater systems. The effect of agitation time on the flocculation was less significant compared to the other two parameters. An agitation time longer than 50 min leads to the gradual destabilization and resuspension of viable MA cells instead of the settlement with the flocs, which prolongs the entire flocculation process.

The validation experiments were conducted under selected optimum conditions to confirm the validity of our statistical and experimental strategies (Table 4). The observed removal efficiency of MA cells ranged from 93.8 to 94.7 %. The deviations between the experimental and predicted values ranged from 0.5 to 2.1. The confirmatory experiments demonstrated that the model prediction was in good accordance with the experimental data.

Variation of MA density in different growth phases

The variations of MA density during 72 h in different growth phases are shown in Fig. 5. Compared to the control samples, the dosing of flocculants showed significant negative effect on the density of MA in all treatments. During the stationary phase, the MA density decreased to $2.82\pm0.82\times10^6$ cells mL^{-1} after 1 h of flocculation with the high initial density. In the controls, the MA density showed no significant change ($p>0.05$). During the logarithmic phases, MA cells grew rapidly in the controls while complete flocculation was achieved within 0.5 h. MA density in the controls significantly increased to $1.14\pm0.06\times10^6$ and $2.35\pm0.04\times10^7$ cells mL^{-1}
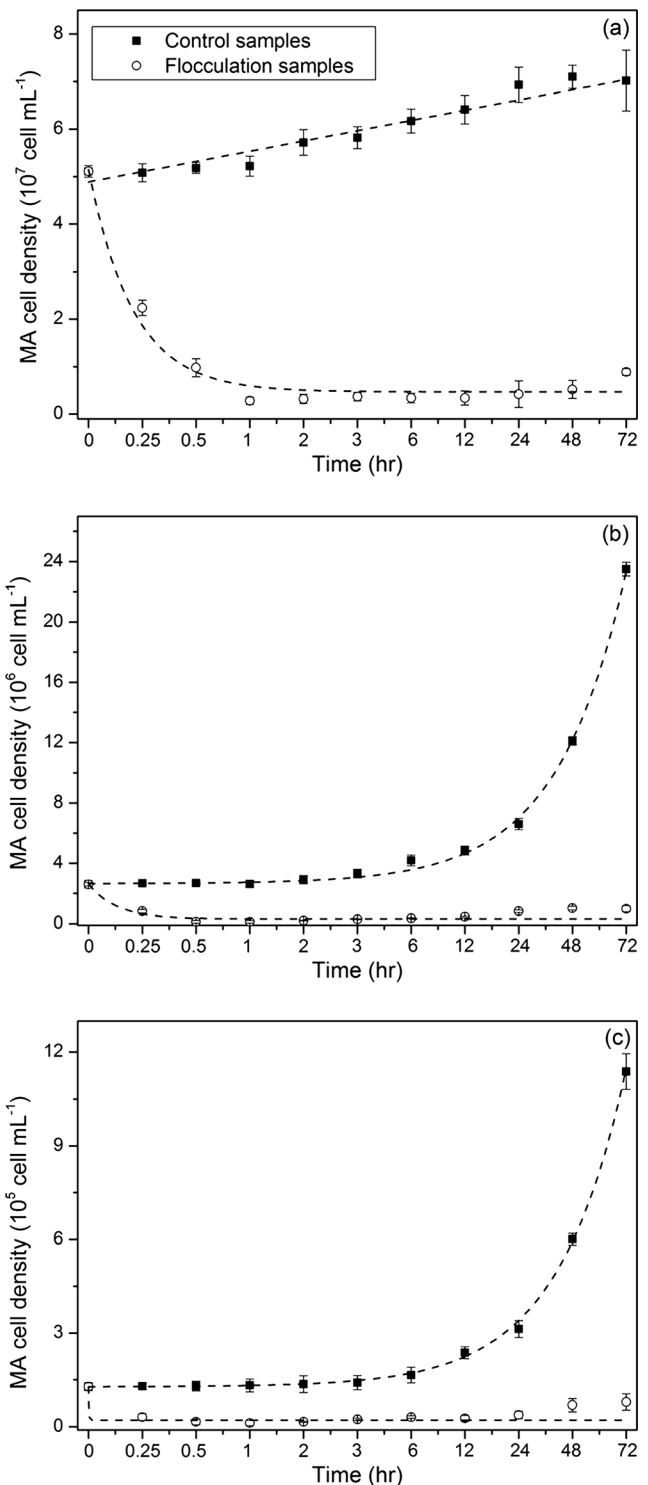

Fig. 5 Variation of *Microcystis aeruginosa* cell density over time: a with high initial cell density, b with medium initial cell density, and c with low initial cell density

after 72 h with the low and medium initial densities, respectively ($p<0.05$), and the density in the flocculation samples significantly decreased to $1.26\pm0.86\times10^4$ and $1.25\pm0.81\times10^5$ cells mL^{-1} at the end of the flocculation process,

respectively ($p<0.05$). A slight increase of MA density was observed in all the flocculation samples after 24 h of incubation.

The rapid decrease of MA density after 0.5 h of flocculation indicated that the CTS/NMMT nanocomposite removed over 95 % MA cells in all treatments and effectively inhibited the growth of MA cells. The SEM images shown in Fig. 6 confirmed that the MA cells in the control had an ovoid, intact, smooth, and plump shape with an average diameter of 3 μm. The morphology of MA cells showed no major alteration and their spherical shape was still kept shortly after the flocculation, while the MA cells were connected by long-chain polymers and their surfaces were coated with thick layers. After 72 h of floc storage, the MA cells became distorted and flattened. The surfaces of most cracked cells were rough and the cell membrane was lysed. The flocs mainly contained the deformed cell walls together with CTS-MA colloid as agglutinants. The bridging effect of the polymer effectively aggregates the cells in flocs, while the severe cell disruption and the membrane damage should also be attributed to the presence of CTS during the floc storage process (Liu et al. 2004a).

Variation of intracellular MC-LR concentrations in different growth phases

The variations of intracellular MC-LR concentrations during 72 h in different growth phases are shown in Fig. 7a–c. The intracellular MC-LR concentrations in the controls exhibited no significant change when the MA cells were in the stationary phase ($p>0.05$), but showed a significant increase from 5.3 ± 1.1 to 35.1 ± 0.2 μg L^{-1} and from 72.6 ± 10.2 to 312.0 ± 5.0 μg L^{-1} with the low and medium initial MA densities, respectively ($p<0.05$), when the MA cells were in the logarithmic phases. In the flocculation samples, the logarithmic-growing MA cells demonstrated a similar trend as the sample

in the stationary phase in releasing the intracellular MC-LR. Within 1 h, the intracellular MC-LR concentration with the low and medium initial densities significantly decreased to 0.2 ± 0.1 and 4.6 ± 3.1 μg L^{-1}, respectively ($p<0.05$), while it took 12 h for the intracellular MC-LR concentration with the high initial density to decrease significantly to 15.3 ± 8.1 μg L^{-1} ($p<0.05$). The intracellular MC-LR concentration remained constant during the floc storage process afterwards ($p>0.05$).

As shown in Fig. 7d–f, MA cells possessed higher intracellular MC-LR concentration in the controls during logarithmic growth phases. The producing ability of intracellular MC-LR decreased with medium and high initial densities in the controls during 72 h of incubation. With the low initial density, MA cells produced the highest concentration of intracellular MC-LR and its producing ability of intracellular MC-LR showed an increasing trend. By analyzing the yields of intracellular MC-LR in the flocculation samples, the similar decreasing trends were observed in all treatments. The producing ability of intracellular MC-LR in the flocculation samples was significantly weaker than that in the controls ($p<0.05$ for each comparison).

The measurement of the intracellular MC-LR concentration can be used as a secondary parameter to measure cell concentration (Drikas et al. 2001). The values of intracellular MC-LR concentration matched well with the results obtained in the density measurement. The cell quota of MCs increases linearly with the specific growth rate before reaching a maximum (Long et al. 2001). The observations in our study supported the widely held view that the intracellular MC-LR concentration would be higher with a more favorable condition for MA growth (Hu et al. 2014). The presence of CTS/ NMMT showed a negative effect on the yield of intracellular MC-LR of MA cells, which indicated the cell damage and the leakage of intracellular MC-LR.
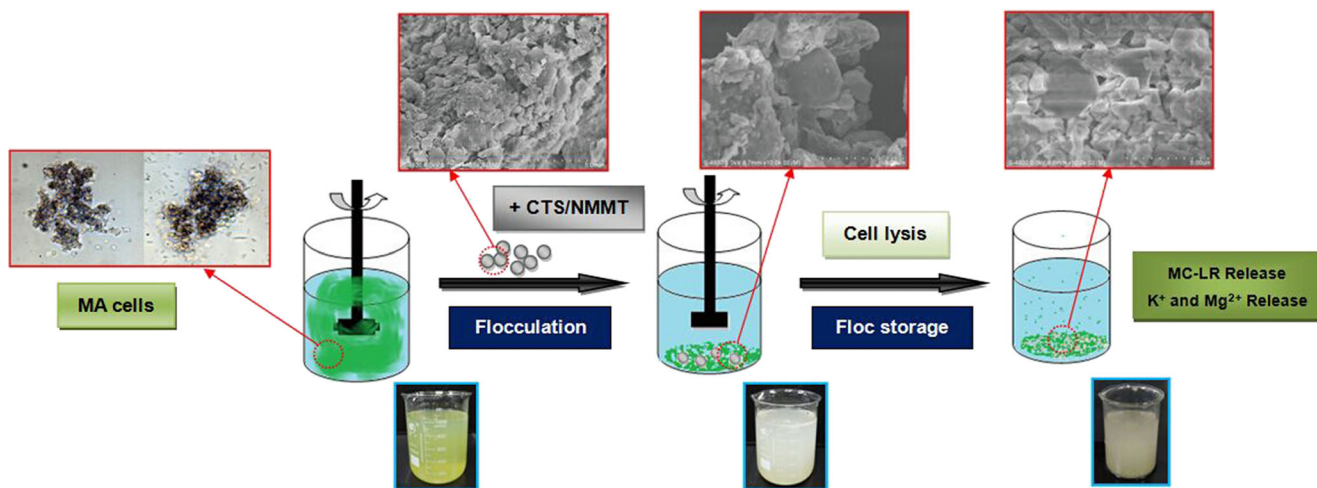

Fig. 6 Schema of the flocculation and floc storage process

Variation of extracellular MC-LR concentrations and K$^+$ and Mg^{2+} release in different growth phases

The variations of extracellular MC-LR concentrations during 72 h in different growth phases are shown in Fig. 8a–c. The extracellular MC-LR concentrations in the controls increased gradually from 1.3±0.4 to 3.4±0.7 μg L^{-1} and from 6.6±1.1 to 10.1±1.0 μg L^{-1} with the low and medium initial MA densities, respectively, but showed a significant increase from

47.8±2.2 to 110.1±12.4 μg L^{-1} with the high initial MA density. In the flocculation samples, the decreasing trends of the extracellular MC-LR concentration were similar in all treatments and the adsorption of 90 % extracellular MC-LR was achieved within 1 h. The extracellular MC-LR concentration showed no significant changes during the floc storage process till 12 h ($p>0.05$) and slightly increased afterwards.

Although the integrity of MA cells was recorded by SEM analysis, the release of K$^+$ and Mg^{2+}, which was the indicator
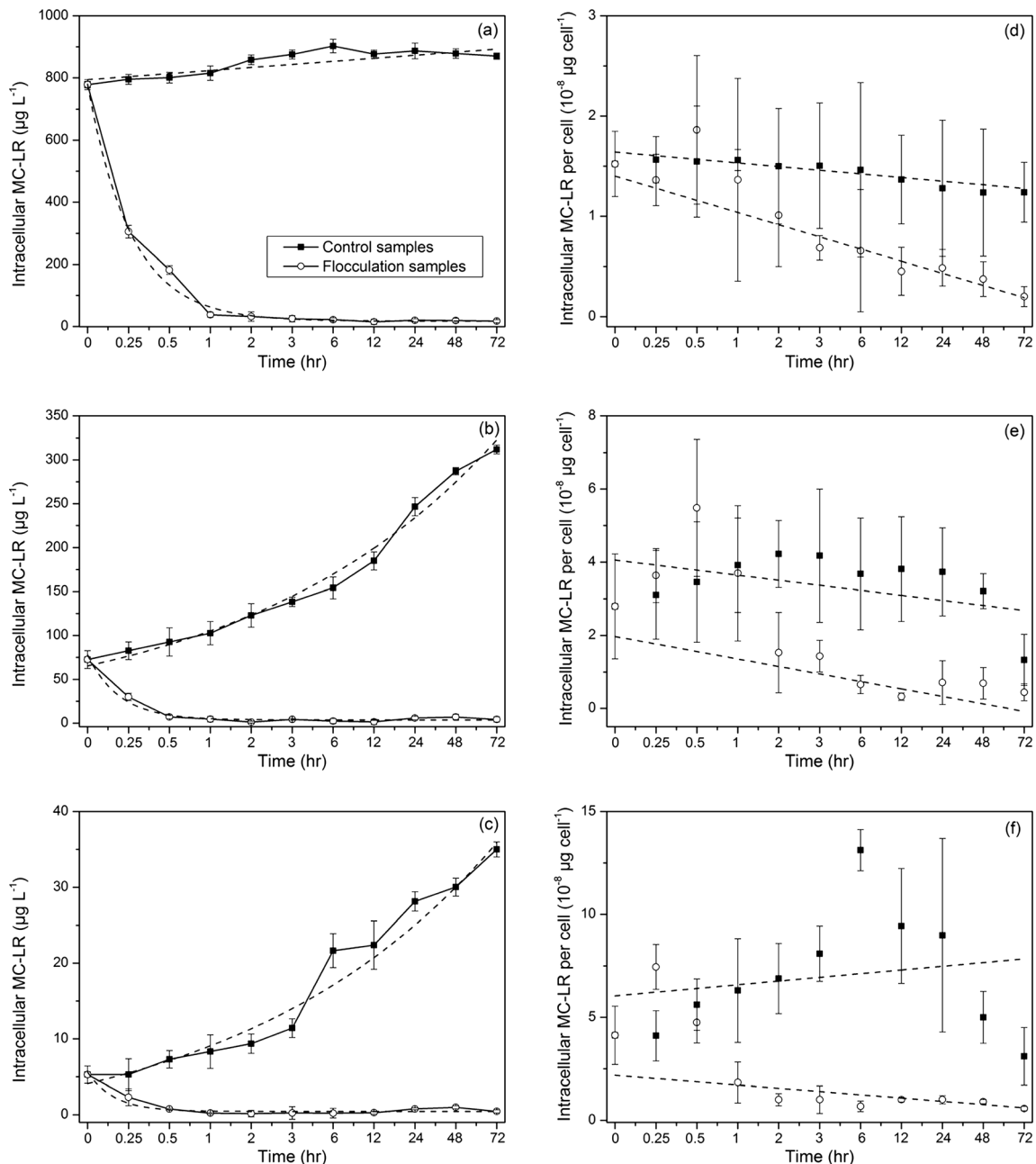

Fig. 7 Variation of intracellular MC-LR concentration and MC-LR yield per MA cell over time: a intracellular MC-LR concentration with high initial cell density, b intracellular MC-LR concentration with medium initial cell density, c intracellular MC-LR concentration with low initial cell density, d MC-LR yield with high initial cell density, e MC-LR yield with medium initial cell density, and f MC-LR yield with low initial cell density

of cell integrity and membrane function, was investigated to further evaluate the cell damage caused by the flocculation as illustrated in Fig. 8d–f. The K^+ and Mg^{2+} adsorption capacities of CTS/NMMT were denied by comparison of CTS/NMMT-added samples with crude extract samples. It can be clearly observed that the release of K^+ and Mg^{2+} showed no remarkable changes during the first 12 h and significantly increased afterwards ($p < 0.05$ for each comparison). A lower MA initial

density was accompanied with a higher release of K^+ and Mg^{2+}.

The release of K^+ from ruptured cell membranes was an important indicator of MA cell lysis (Ma et al. 2012). The release of Mg^{2+} can be regarded as the indication of the damage degree of lipopolysaccharide (LPS) layers, which are the first sites of destruction resulting in increases in cell permeability and eventually lysis (Zhang et al. 2011). The analysis of K^+ and Mg^{2+} release in this study excluded the influence of
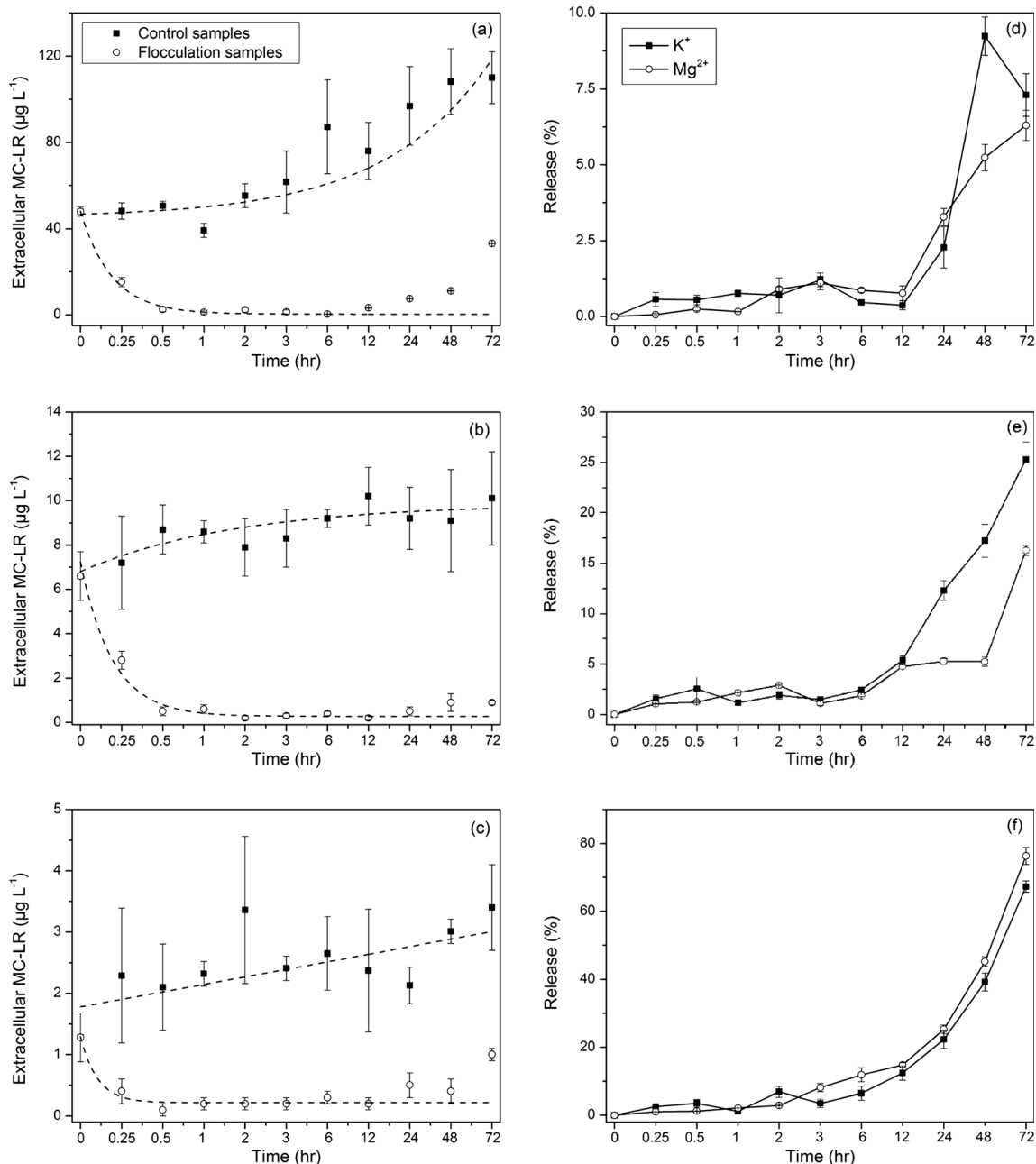

Fig. 8 Variation of extracellular MC-LR concentration and release of K^+ and Mg^{2+} over time: a extracellular MC-LR concentration with high initial cell density, b extracellular MC-LR concentration with medium initial cell density, c extracellular MC-LR concentration with low initial cell density, d release of K^+ and Mg^{2+} with high initial cell density, e release of K^+ and Mg^{2+} with medium initial cell density, and f release of K^+ and Mg^{2+} with low initial cell density

the natural cell lysis and transportation of MC-LR across the cell membrane. No significant cell damage was shown during the flocculation process. A possible explanation for the slight initial leakage is that the cell lysis is intensified and the organelles of some MA cells may suffer the mechanical damage from the continuous stirring during the flocculation.

Chitosan performed firstly as the protective shield of cells and then interacted with the colloid membrane. After further storage, the cell impurities mixed with chitosan degraded gradually and led to the entire cell lysis. The noticeable increase of K^+ and Mg^{2+} release after 12 h indicated that the protection function of chitosan weakened and even vanished. Moreover, the absorption of the extracellular polymeric substances (EPS) by CTS destroyed the protective shield formed by EPS with prolonged storage time (Xu et al. 2013). It was further proposed that the leakage of intercellular substances and the damage of cellular membranes caused the death of MA cells (Pei et al. 2014). A similar trend of $AlCl_3$ flocculant was discovered much slower (48 h) in a previous study (Sun et al. 2012). During the floc storage process, the MA cell lysis, the major mechanism responsible for the increase of extracellular MC-LR in water, was likely accelerated by the deformation of the long-chain polymer (Zhou et al. 2013).

Toxin release during the breakdown of MA cells in the floc storage process should be taken into consideration, and the timely recovery of flocs should be the focal point in the water treatment process. The increase of extracellular MC-LR normally indicates the breakdown of cells and the leakage of toxins (Drikas et al. 2001). During the flocculation process, the amount of intracellular MC-LR excretion could be ignored while most cells remained intact. The maximum detention time of MC-LR in MA cells trapped in the flocs was assessed to be 12 h. A number of intracellular MC-LR were released into the supernatant after that.

However, the decrease of intracellular MC-LR did not bring to the significant increase of extracellular MC-LR. The desirable MC-LR adsorption capacity of NMMT and CTS has been reported in previous studies (Pei et al. 2014; Wang et al. 2014). Nevertheless, the extracellular toxins are not readily removed while the cells remain intact (Sun et al. 2013). Despite the fact that the extracellular MC-LR concentration showed a slight increase after 12 h in all the treatments, which might be the consequence of the release of intracellular MC-LR due to the increased cell permeability after the lysis, the decreased total MC-LR concentration indicated the effective adsorptive removal of extracellular MC-LR by CTS/NMMT during the flocculation and floc storage process.

According to the desorption method reported in our previous study (Wang et al. 2014), the flocs with the high initial density after 72 h of storage were collected for MC-LR desorption experiments using 0.1 M NaOH as eluting medium.

The contribution of flocs to the extracellular MC-LR adsorptive removal was validated by the comparison of MC-LR concentration desorbed from the flocs (606.3 ± 2.5 µg L^{-1}) with the variance of total MC-LR concentrations in flocculation and control (929.2 ± 12.0 µg L^{-1}). The results suggested that a small number of cells in flocs remained intact and were still in a healthy state with normal viability and producing ability of intracellular MC-LR.

In view of the above findings, the application of the CTS/NMMT flocculant aggregated MA cells as flocs and served as cell protection during 0.5 h of flocculation. Meanwhile, the physical contact caused little cell damage and released a minimal amount of intracellular MCs. As CTS degraded gradually during the floc storage process, the cell lysis and membrane damage were aggravated. After 12 h of floc storage, the remarkable increase of K^+ and Mg^{2+} release indicated that CTS/NMMT damaged most MA cells in the flocs and liberated the intracellular MC-LR, but also helped remove the extracellular MCs in water at the same time.

Conclusions

The MA flocculation efficiency of the CTS/NMMT nanocomposite was found to reach a peak of 94.9 % with the initial density representing the logarithmic growth phase. Based on the RSM approach using the Box–Behnken experimental design and fitting the quadratic statistical model, the optimum flocculation conditions were obtained as CTS/NMMT content 300–320 mg L^{-1}, weight ratio of NMMT to CTS 14–16, and agitation time 16–50 min. During the flocculation process, CTS/NMMT aggregated MA cells as flocs and served as protection shield for cells. The cell integrity was slightly damaged by the mechanical actions rather than by the flocculant. The extracellular and intracellular MC-LR decreased remarkably, and the yield of intracellular MC-LR showed a decreasing trend in the flocculation samples. The cell lysis and membrane damage were aggravated during the floc storage process. The noticeable increase of K^+ and Mg^{2+} release indicated that CTS/NMMT damaged most MA cells in the flocs and liberated the intracellular MC-LR. Meanwhile, CTS/NMMT assisted the adsorptive removal of extracellular MC-LR in water. The flocs should be timely treated within 12 h to prevent the leakage of MCs.

References

Auta M, Hameed B (2014) Chitosan–clay composite as highly effective and low-cost adsorbent for batch and fixed-bed adsorption of methylene blue. Chem Eng J 237:352–361

Campos A, Vasconcelos V (2010) Molecular mechanisms of microcystin toxicity in animal cells. Int J Mol Sci 11:268–287

Carmichael WW (2001) Health effects of toxin-producing cyanobacteria:"The CyanoHABs". Hum Ecol Risk Assess 7: 1393–1407

Chen C-Y, Chung Y-C (2011) Comparison of acid-soluble and water-soluble chitosan as coagulants in removing bentonite suspensions. Water Air Soil Pollut 217:603–610

Dong C, Chen W, Liu C (2014) Flocculation of algal cells by amphoteric chitosan-based flocculant. Bioresour Technol 170: 239–247

Drikas M, Chow CW, House J, Burch MD (2001) Using coagulation, flocculation, and settling to remote toxic cyanobacteria. J Am Water Works Assoc 93:100–111

Farid MS, Shariati A, Badakhshan A, Anvaripour B (2013) Using nano-chitosan for harvesting microalga Nannochloropsis sp. Bioresour Technol 131:555–559

Ho L et al (2012) Fate of cyanobacteria and their metabolites during water treatment sludge management processes. Sci Total Environ 424: 232–238

Hu X et al (2014) Effects of d-menthol stress on the growth of and microcystin release by the freshwater cyanobacterium Microcystis aeruginosa FACHB-905. Chemosphere 113:30–35

Hua Z, Gang P, Hao C, Xianzheng Y (2006) Removal of cyanobacterial blooms in Taihu Lake using local soils II. Effective removal of Microcystis aeruginosa using local soils and sediments modified by chitosan. Environ Pollut 141(2):201–205

Imandi SB, Bandaru VR, Somalanka SR, Garapati HR (2007) Optimization of medium constituents for the production of citric acid from byproduct glycerol using Doehlert experimental design. Enzym Microb Technol 40:1367–1372

Jančula D, Maršálek B (2011) Critical review of actually available chemical compounds for prevention and management of cyanobacterial blooms. Chemosphere 85:1415–1422

Kumar MS, Phanikumar B (2013) Response surface modelling of Cr6+ adsorption from aqueous solution by neem bark powder: Box–Behnken experimental approach. Environ Sci Pollut Res 20:1327–1343

Li X et al (2015) The fate of Microcystis aeruginosa cells during the ferric chloride coagulation and flocs storage processes. Environ Technol 36(7):920–928

Liu H, Du Y, Wang X, Sun L (2004a) Chitosan kills bacteria through cell membrane damage. Int J Food Microbiol 95:147–155

Liu HL, Lan YW, Cheng YC (2004b) Optimal production of sulphuric acid by Thiobacillus thiooxidans using response surface methodology. Process Biochem 39:1953–1961. doi:10.1016/j.procbio.2003.09.018

Long BM, Jones GJ, Orr PT (2001) Cellular microcystin content in N-limited Microcystis aeruginosa can be predicted from growth rate. Appl Environ Microbiol 67:278–283

Ma M, Liu R, Liu H, Qu J (2012) Chlorination of Microcystis aeruginosa suspension: cell lysis, toxin release and degradation. J Hazard Mater 217:279–285

Pan G, Zhang M-M, Chen H, Zou H, Yan H (2006a) Removal of cyanobacterial blooms in Taihu Lake using local soils. I. Equilibrium and kinetic screening on the flocculation of Microcystis aeruginosa using commercially available clays and minerals. Environ Pollut 141:195–200

Pan G, Zou H, Chen H, Yuan X (2006b) Removal of harmful cyanobacterial blooms in Taihu Lake using local soils III. Factors affecting the removal efficiency and an in situ field experiment using chitosan-modified local soils. Environ Pollut 141:206–212

Pei H-Y, Ma C-X, Hu W-R, Sun F (2014) The behaviors of Microcystis aeruginosa cells and extracellular microcystins during chitosan flocculation and flocs storage processes. Bioresour Technol 151: 314–322

Polyak Y, Zaytseva T, Medvedeva N (2013) Response of toxic cyanobacterium Microcystis aeruginosa to environmental pollution. Water Air Soil Pollut 224:1–14

Renault F, Sancey B, Badot P-M, Crini G (2009) Chitosan for coagulation/flocculation processes—an eco-friendly approach. Eur Polym J 45:1337–1348

Shao J et al (2012) Physiological responses of Microcystis aeruginosa NIES-843 (cyanobacterium) under the stress of chitosan modified kaolinite (CMK) loading. Ecotoxicology 21:698–704

Sun F, Pei H-Y, Hu W-R, Ma C-X (2012) The lysis of Microcystis aeruginosa in AlCl$_3$ coagulation and sedimentation processes. Chem Eng J 193:196–202

Sun F, Pei H-Y, Hu W-R, Li X-Q, Ma C-X, Pei R-T (2013) The cell damage of Microcystis aeruginosa in PACl coagulation and floc storage processes. Sep Purif Technol 115:123–128

Thirumavalavan M, Hu Y-L, Lee J-F (2012) Effects of humic acid and suspended soils on adsorption and photo-degradation of microcystin-LR onto samples from Taiwan reservoirs and rivers. J Hazard Mater 217:323–329

Venrick E (1978) How many cells to count. Phytoplankton manual. UNESCO, Paris, pp 167–180

Wan Ngah W, Teong L, Hanafiah M (2011) Adsorption of dyes and heavy metal ions by chitosan composites: a review. Carbohydr Polym 83: 1446–1456

Wang L, Wang A (2007) Adsorption characteristics of Congo Red onto the chitosan/montmorillonite nanocomposite. J Hazard Mater 147: 979–985

Wang ZY, Wang C, Wang PF, Qian J, Hou J, Ao YH (2014) Process optimization for microcystin-LR adsorption onto nano-sized montmorillonite K10: application of response surface methodology. Water Air Soil Pollut 225(9):1–18. doi:10.1007/S11270-014-2124-5

Xu H, Cai H, Yu G, Jiang H (2013) Insights into extracellular polymeric substances of cyanobacterium Microcystis aeruginosa using fractionation procedure and parallel factor analysis. Water Res 47: 2005–2014

Yan H, Gong A, He H, Zhou J, Wei Y, Lv L (2006) Adsorption of microcystins by carbon nanotubes. Chemosphere 62:142–148

Yetilmezsoy K, Saral A (2007) Stochastic modeling approaches based on neural network and linear-nonlinear regression techniques for the determination of single droplet collection efficiency of countercurrent spray towers. Environ Model Assess 12:13–26. doi:10.1007/s10666-006-9048-4

Zeng D, Wu J, Kennedy JF (2008) Application of a chitosan flocculant to water treatment. Carbohydr Polym 71:135–139

Zhang YQ, Wu QP, Zhang JM, Yang XH (2011) Effects of ozone on membrane permeability and ultrastructure in Pseudomonas aeruginosa. J Appl Microbiol 111:1006–1015. doi:10.1111/j.1365-2672.2011.05113.x

Zhang Z, Pang Q, Li M, Zheng H, Chen H, Chen K (2015) Optimization of the condition for adsorption of gallic acid by Aspergillus oryzae mycelia using Box-Behnken design. Environ Sci Pollut Res 22: 1085–1094

Zhou S, Shao Y, Gao N, Deng Y, Qiao J, Ou H, Deng J (2013) Effects of different algaecides on the photosynthetic capacity, cell integrity and microcystin-LR release of Microcystis aeruginosa. Sci Total Environ 463–464:111–119. doi:10.1016/j.scitotenv.2013.05.064